

Clustering in dynamical dark energy: observational constraints from DESI, CMB, and supernovae

YUHANG YANG ,^{1,2} QINGQING WANG ,^{1,2,3} XIN REN ,^{1,2} EMMANUEL N. SARIDAKIS ,^{4,2,5} AND YI-FU CAI ,^{1,2}¹Department of Astronomy, School of Physical Sciences, University of Science and Technology of China, Hefei 230026, China²CAS Key Laboratory for Research in Galaxies and Cosmology, School of Astronomy and Space Science, University of Science and Technology of China, Hefei 230026, China³Kavli IPMU (WPI), UTIAS, The University of Tokyo, Kashiwa, Chiba 277-8583, Japan⁴National Observatory of Athens, Lofos Nymfon 11852, Greece⁵Departamento de Matemáticas, Universidad Católica del Norte, Avda. Angamos 0610, Casilla 1280, Antofagasta, Chile

ABSTRACT

We investigate the clustering properties of dynamical dark energy using the latest cosmological observations. We describe the dark energy perturbation within two complementary frameworks, namely the Parameterized Post-Friedmann (PPF) approach and the Effective Field Theory (EFT) of dark energy. Using DESI DR2 baryon acoustic oscillations together with Planck 2018 CMB data and the Union3 supernova sample, we constrain the effective sound speed of dark energy in both the w CDM and w_0w_a CDM backgrounds. Within the PPF description, the sound speed remains unconstrained for w CDM, while for the w_0w_a CDM case we obtain $\log_{10} c_s^2 = -3.00^{+2.9}_{-0.99}$. Additionally, in the EFT framework, both models favor a small sound speed, with a mean value $c_s^2 \simeq 0.3\text{--}0.4$ but with significant uncertainties. For dynamical dark energy, the reconstructed equation of state clearly exhibits a quintom-B behavior, and its deviation from Λ CDM reaches 3.42σ , rising to 3.63σ when PPF perturbations are included and reducing to 3.19σ in the EFT case. Finally, model comparison using information criteria shows that the w_0w_a CDM model with a smooth, non-clustering dark energy component ($c_s^2 = 1$) is preferred by AIC, whereas BIC favors Λ CDM. In summary, current data indicate a mild preference for dynamical dark energy but no evidence for significant clustering, which implies the need for future high-precision observations to probe the perturbative behavior more definitively.

1. INTRODUCTION

The discovery of the Universe's accelerated expansion in 1998, via Type Ia supernovae (SNe) Riess et al. (1998); Perlmutter et al. (1999), established the cosmological constant Λ dark energy as the cornerstone of the standard Λ CDM model. Recently, observations from the Dark Energy Spectroscopic Instrument (DESI) data release 2 (DR2) have presented a direct challenge to this paradigm Abdul Karim et al. (2025) by using w_0w_a or Chevallier-Polarski-Linder (CPL) parametrization for dark energy Chevallier & Polarski (2001); Linder (2003). Reporting deviations from Λ CDM at the $2.8\text{--}4.2\sigma$ level, depending on the SNe sample used, DESI data strongly hints that dark energy may be dynamical, signaling new physics beyond the standard cosmological model.

Intriguingly, DESI results strongly favor a quintom dark energy model whose equation of state parame-

ter w crosses the cosmological constant boundary $w = -1$ (also dubbed the phantom divide) during cosmic evolution Abdul Karim et al. (2025). More specifically, quintom-B dark energy, w exhibits phantom behavior ($w < -1$) at early times and evolves toward quintessence-like behavior ($w > -1$) at late epochs Feng et al. (2005); Hu (2005); Ratra & Peebles (1988); Wetterich (1988); Caldwell (2002). This crossing behavior is robust, as it remains consistent across different dark energy parameterizations and is also recovered in non-parametric reconstructions Lodha et al. (2025); Gu et al. (2025); Yang et al. (2024). This unexpected result has inspired the reanalysis of the SNe data to examine the favor of evolving dark energy Efstathiou (2025); Popovic et al. (2025), and some theoretical models to explain the quintom evolution Yang et al. (2025a); Giarè et al. (2024); Wolf et al. (2025); Basilakos et al. (2025); Li et al. (2024, 2025); Chaussidon et al. (2025); Luciano et al. (2026); Goh & Taylor (2025); Ye et al. (2025). However, as reviewed in Cai et al. (2010, 2025), for basic single-field dark energy models or perfect fluid dark en-

ergy models, they suffer from divergence problems at the perturbative level when crossing phantom divide which is also known as the No-Go theorem of quintom dark energy [Vikman \(2005\)](#); [Deffayet et al. \(2010\)](#); [Chimento et al. \(2009\)](#); [Cai et al. \(2010\)](#). Theoretically, multi-field theory or modified gravity like Henderski theory can either define a finite sound speed or modify the dispersion relation to avoid the divergence problem, thus give a healthy theory interpretation of quintom dark energy model [Guo et al. \(2005\)](#); [Zhang et al. \(2006\)](#); [Horndeski \(1974\)](#).

The behavior of dark energy perturbations has recently gained increasing importance due to mounting observational tensions and theoretical consistency requirements. Given that DESI DR2 favors dynamical models such as quintom-B, assessing their perturbation behavior becomes essential. In particular, the persistent S_8 (growth) tension, reflecting the mismatch between the amplitude of matter clustering inferred from the CMB and low-redshift probes, suggests that the microphysical properties of dark energy may influence structure formation more strongly than in Λ CDM [Di Valentino et al. \(2021\)](#). Moreover, dynamical dark energy models, especially those with w crossing -1 , often exhibit perturbative instabilities or pathological sound speeds that can amplify or suppress density fluctuations. Understanding the clustering behavior of dark energy is therefore essential for assessing the viability of dynamical equation-of-state models and for quantifying their impact on growth observables, cosmic structure formation, and the evolution of perturbations at late times.

Since the perturbation of dark energy is of great significance in the construction of dark energy models, it is also very necessary to take into account the perturbation of dark energy when conducting cosmological analyses [Fang et al. \(2008\)](#); [Zhao et al. \(2005\)](#); [Xia et al. \(2008\)](#); [Dinda & Banerjee \(2024\)](#); [Bhattacharyya et al. \(2019\)](#). In addition to constructing a reasonable model theoretically, developing a set of technical methods to handle divergence within the framework of parameterized dark energy is also very necessary. One is the Parameterized Post-Friedmann (PPF) description, which offers a consistent approach to modeling dark energy perturbations as a non-interacting fluid [Fang et al. \(2008\)](#); [Hu \(2008\)](#). A key feature of this framework is that it assumes that dark energy perturbations only matter on large scales. Its principal advantage lies in dealing with the divergence of perturbations when the equation of state w crosses the phantom divide, which is achieved by defining a new variable that remains regular across

the phantom divide, enabling stable and observationally viable predictions.

Another appropriate way to handle dark energy perturbations is to consider dark energy as a scalar field or as a consequence of modifying the theory of gravity, which can be uniformly described through the effective field theory (EFT) of dark energy [Gubitosi et al. \(2013\)](#); [Bloomfield et al. \(2013\)](#); [Creminelli et al. \(2009\)](#); [Park et al. \(2010\)](#); [Gleyzes et al. \(2013\)](#); [Li et al. \(2018\)](#); [Yan et al. \(2020\)](#); [Ren et al. \(2022\)](#); [Yang et al. \(2025b\)](#). By imposing reasonable restrictions on the functions of EFT, we can also obtain a dark energy theory without any divergence problems [De Felice et al. \(2017\)](#).

One of the most important parameters for describing dark energy perturbations is the speed of sound of dark energy c_s^2 , for example, the small value of c_s^2 can lead to the clustering effect of dark energy, thus leave an imprint on the observables [Batista \(2021\)](#); [Xia et al. \(2008\)](#); [Basse et al. \(2012\)](#); [Takada \(2006\)](#); [Kunz et al. \(2015\)](#). From an analytical perspective, the clustering behavior of dark energy is largely governed by its effective sound speed c_s^2 and the associated comoving Jeans scale $k_J^2 \sim a^2 H^2 / c_s^2$. For models with $c_s^2 \simeq 1$, dark energy remains smooth on sub-horizon scales and contributes negligibly to structure growth, whereas a small sound speed ($c_s^2 \ll 1$) suppresses the Jeans scale, allowing dark energy to cluster and modify the evolution of matter perturbations. However, when $w < -1$, the effective sound speed can become negative or ill-defined in many parameterized models, triggering gradient instabilities in k^2 modes unless regulated by a PPF or EFT prescription. These analytical considerations underline the importance of treating dark energy perturbations consistently, especially for dynamical equation of state models that approach or cross the phantom divide.

The analysis of clustering dark energy by the Planck team indicates that c_s^2 is unconstrained [Ade et al. \(2016\)](#). In this manuscript, we will use the latest observations to examine the clustering effect of dynamical dark energy. This manuscript is structured as follows. Section 2 reviews the PPF framework for dark energy and examines the impact of its perturbations on cosmological observables. In Section 3 we briefly introduce the EFT of dark energy and its phenomenological parameterization. Section 4 presents the datasets and methodology, followed by a discussion of the main results. Our conclusions are summarized in Section 5.

2. PPF DESCRIPTION FOR THE DARK ENERGY PERTURBATIONS

Generally, we treat dark energy as an additional non-interacting fluid (along with cold dark matter (CDM)

and radiation) with equation of state $w = p_{\text{de}}/\rho_{\text{de}}$. The perturbations of dark energy can be fully described by four independent perturbation variables, density fluctuation $\delta\rho_{\text{de}}$, bulk velocity v_{de} , pressure fluctuation δp_{de} and anisotropic stress Π_{de} . It is more convenient to introduce the density contrast $\delta_{\text{de}} \equiv \delta\rho_{\text{de}}/\rho_{\text{de}}$ and the velocity perturbations $\theta_{\text{de}} \equiv \partial_i v_{\text{de}}^i$, while at linear perturbation level the anisotropic perturbations are always assumed to be zero.

In the general case, the dark energy perturbations are not adiabatic, and can produce entropy, thus they are called entropic perturbations or isocurvature perturbations. In an arbitrary gauge, the relation between dark energy δp_{de} and $\delta\rho_{\text{de}}$ can be expressed as

$$\delta p_{\text{de}} = c_s^2 \delta\rho_{\text{de}} + 3(1+w)\rho_{\text{de}} \left(c_s^2 - c_a^2 \right) \frac{v_{\text{de}}}{k_H}, \quad (1)$$

$k_H = k/aH$ with k the wave number in the Fourier space, H the Hubble parameter, $c_s^2 = \delta p_{\text{de}}^{\text{rest}}/\delta\rho_{\text{de}}^{\text{rest}}$ is the sound speed in the dark energy rest frame and $c_a^2 = \dot{\rho}_{\text{de}}/\dot{p}_{\text{de}}$ is the adiabatic sound speed, where dots represent the derivatives with respect to cosmic time.

As one can see, when w crosses -1 , the c_a^2 will diverge, leading to the instability of perturbations [Vikman \(2005\)](#); [Deffayet et al. \(2010\)](#); [Chimento et al. \(2009\)](#). This kind of divergence problems is thoroughly discussed within the No-Go theorem of dark energy [Cai et al. \(2010\)](#). However, instead of discussing how to theoretically avoid such a divergent issue, we focus on how to handle this problem at the technical level, by using the Parameterized Post-Friedmann (PPF) description of dark energy perturbations.

The PPF framework describes dark energy perturbations through a unified dynamical variable Γ , while rigorously preserving energy-momentum conservation [Fang et al. \(2008\)](#); [Hu \(2008\)](#). In PPF analysis, the dark energy density and momentum evolutions are fully determined by the quantities

$$\Gamma \equiv -\frac{4\pi Ga^2}{k^2 \mu_K} \rho_{\text{de}} \delta_{\text{de}}^{\text{rest}} \quad (2)$$

$$S = -\frac{4\pi G}{H^2} \left[f_\zeta(t) (\rho_T + p_T) - \rho_{\text{de}}(1+w) \right] \frac{v_T + k\alpha}{k_H}. \quad (3)$$

Here $\alpha = a(\dot{h} + 6\dot{\eta})/2k^2$, where h is the trace of metric perturbation while η is the scalar shearing potential in synchronous gauge [Ma & Bertschinger \(1995\)](#). Moreover, $\delta_{\text{de}}^{\text{rest}}$ is the density contrast of dark energy at the dark energy rest frame, while the subscript “T” denotes all other components excluding the dark energy. Finally, $\mu_K = 1 - 3K/k^2$ where K is the background curvature and $f_\zeta(t)$ is a function of time only. In the following we

set $\mu_K = 1$, and it is proved that for most purposes it is sufficient to set $f_\zeta = 0$ [Fang et al. \(2008\)](#). Furthermore, the PPF framework assumes that dark energy becomes smooth relative to matter inside a transition scale $c_s k_H = 1$, while exactly conserving energy and momentum locally by taking

$$(1 + c_\Gamma^2 k_H^2) \left[\frac{\dot{\Gamma}}{H} + \Gamma + c_\Gamma^2 k_H^2 \Gamma \right] = S. \quad (4)$$

We mention that for subsequent calculations we impose $c_\Gamma = 0.4c_s$ [Fang et al. \(2008\)](#). With the PPF method, we can solve the full equations at $k_H \rightarrow 0$, and extract the correct evolution for the metric or gravitational potentials. We mention that the dark-energy perturbations will affect the evolution of the gravitational potential, and thereby can produce observable phenomena in the temperature power spectrum of the CMB through the integrated Sachs-Wolfe (ISW) effect.

A commonly used parameterization is the Chevallier-Polarski-Linder (CPL) one [Chevallier & Polarski \(2001\)](#); [Linder \(2003\)](#), which expresses $w(z)$ in terms of the scale factor a to the first order as

$$w(a) = w_0 + w_a(1-a), \quad (5)$$

where w_0 represents the value of w at current time, while $w_0 + w_a$ represents the value at very early universe. We refer to $w_0 w_a$ -parametrized dark-energy models with $c_s^2 = 1$ as $w_0 w_a$ CDM models, while models with constant w (i.e. $w_a = 0$) and $c_s^2 = 1$ as w CDM models. Additionally, we refer to $w_0 w_a$ -parametrized dark energy with arbitrary sound speed and under PPF method as $w_0 w_a$ CDM+PPF one, and similarly models with constant w with an arbitrary sound speed and under the PPF method are referred as w CDM+PPF. Finally, considering dark energy perturbations will lead to the suppression of the TT power spectrum and the matter power spectrum in the low ℓ region, i.e. the large-scale region, however it will have almost no effect on the high ℓ region, i.e. the small-scale region [Fang et al. \(2008\)](#); [Zhao et al. \(2005\)](#).

3. EFFECTIVE FIELD THEORY OF DARK ENERGY

In addition to treating dark energy as a fluid and addressing the divergence issue when w crosses -1 within the PPF framework, dark energy can also be described as a scalar field or as arising from gravitational modifications. The effective field theory (EFT) approach of dark energy offers a unified framework for studying the background and perturbation evolution [Gubitosi et al. \(2013\)](#); [Bloomfield et al. \(2013\)](#); [Creminelli et al. \(2009\)](#); [Park et al. \(2010\)](#); [Gleyzes et al. \(2013\)](#); [Li et al. \(2018\)](#);

Yan et al. (2020); Ren et al. (2022); Yang et al. (2025b), and in particular, a key advantage is that it allows perturbations to be analyzed independently from the back-

$$S = \int d^4x \sqrt{-g} \left[\frac{M_P^2}{2} [1 + \Omega(t)] R - \Lambda(t) - c(t) g^{00} + \frac{M_2^4(t)}{2} (\delta g^{00})^2 - \frac{\bar{M}_1^3(t)}{2} \delta g^{00} \delta K \right. \\ \left. - \frac{\bar{M}_2^2(t)}{2} (\delta K)^2 - \frac{\bar{M}_3^2(t)}{2} \delta K_\nu^\mu \delta K_\mu^\nu + \frac{\hat{M}^2(t)}{2} \delta g^{00} \delta R^{(3)} + m_2(t) \partial_i g^{00} \partial^i g^{00} + \dots \right] \\ + S_m[g_{\mu\nu}, \Psi_m], \quad (6)$$

where M_P is the Planck mass, R is the Ricci scalar, and $\delta g^{00} = g^{00} + 1$ denotes the perturbation of the time-time component of the metric. Furthermore, δK_μ^ν represents the perturbation of the extrinsic curvature, with δK being its trace, and $\delta R^{(3)}$ is the perturbation of the spatial Ricci scalar. The term $S_m[g_{\mu\nu}, \Psi_m]$ describes the action for all matter fields Ψ_m other than dark energy. Note that in the matter sector we assume the validity of the weak equivalence principle (WEP). Consequently, matter fields are minimally coupled to the metric $g_{\mu\nu}$, i.e. we work in the Jordan frame.

The time-dependent functions in the action govern the dark-energy dynamics: $\Lambda(t)$ and $c(t)$ affect exclusively the background evolution, while $\Omega(t)$ parameterizes a non-minimal coupling between the scalar field and gravity. The remaining functions, including $M_2(t)$, $\bar{M}_1(t)$, $\bar{M}_2^2(t)$, $\bar{M}_3(t)$, $\hat{M}(t)$, and $m_2(t)$, primarily affect the behavior of perturbations. The specific forms of all the above functions are determined by the underlying covariant theory of dark energy upon which the EFT is built.

Since the landscape of dark energy theories is vast, and examining each one individually is impractical, we employ a parametric approach within the EFT framework, known as the α -basis Bellini & Sawicki (2014); Hu et al. (2014). This formalism is designed to capture the key physical properties of the broad Horndeski class of theories Horndeski (1974). Within this parameterization, deviations from General Relativity are characterized by four time-dependent phenomenological functions, namely $\alpha_M(t)$, $\alpha_B(t)$, $\alpha_K(t)$, and $\alpha_T(t)$, defined as

$$\alpha_M \equiv \frac{d \ln M_*^2}{d \ln a}, \quad \alpha_B \equiv -\frac{M_P^2 \dot{\Omega} + \bar{M}_1^3}{H M_*^2}, \quad (7) \\ \alpha_K \equiv \frac{2c + 4M_2^4}{H^2 M_*^2}, \quad \alpha_T \equiv c_T^2 - 1 = \frac{M_3^2}{M_*^2},$$

where $M_*^2(t) = M_P^2 [1 + \Omega(t)] - \bar{M}_3^2$ is the effective Planck mass, and c_T is the speed of propagation of tensor modes, or equivalently, of gravitational waves (GWs).

ground. In unitary gauge, the general action for the EFT of dark energy can be written as

The function $\alpha_M(t)$, known as the running Planck mass, characterizes the time evolution of the effective Planck mass M_* . Moreover, the braiding function α_B describes the mixing between the metric and the dark energy field, while the kineticity term α_K affects the kinetic energy of the scalar field and affects the conditions that are necessary to avoid a scalar ghost. Lastly, the tensor speed excess α_T quantifies the deviation of the gravitational wave speed c_T from the speed of light. Following the joint detection of GW170817 and its electromagnetic counterpart GRB170817A Abbott et al. (2017), which constrains $c_T - 1 \lesssim 10^{-15}$, in our analysis we set $\alpha_T = 0$.

Similarly to the instability associated with crossing the phantom divide, certain conditions must be imposed on the α functions to avoid ghost or strong coupling instabilities Sbisà (2015). For instance, to prevent ghost instabilities, we require $D \equiv \alpha_K + \frac{3}{2} \alpha_B > 0$ Cline et al. (2004); Carroll et al. (2003); Gümrükçüoğlu et al. (2016). Additionally, to avoid gradient instabilities, the squared sound speed must satisfy $c_s^2 > 0$ De Felice et al. (2017), where c_s^2 can be directly calculated as Bellini & Sawicki (2014)

$$c_s^2 = \frac{\alpha_B - 2}{H^2 D} \left[\dot{H} - \frac{1}{2} H^2 \alpha_B (1 + \alpha_T) - H^2 (\alpha_M - \alpha_T) \right. \\ \left. - H \dot{\alpha}_B + \rho_m + p_m \right]. \quad (8)$$

Specifically, in our analysis, we strictly require $0 < c_s^2 \leq 1$ to ensure a physically viable sound speed. However, since the α_i functions, where $i \in \{M, B, K\}$, primarily govern the perturbations, a complete cosmological evolution also requires a specification of the background expansion history. For this purpose, we assume a w CDM or $w_0 w_a$ CDM background, calling them w CDM+EFT or $w_0 w_a$ CDM+EFT, respectively. Furthermore, we adopt the commonly used parameterization for the α functions:

$$\alpha_i(t) = c_i \Omega_{de}(t), \quad (9)$$

with $\Omega_{\text{de}}(t)$ the dark-energy density parameter, and c_i constant free parameters Pujolas et al. (2011); Barreira et al. (2014); Bellini & Zumalacárregui (2015). This parameterization naturally ensures that the effect of dark energy becomes negligible in the early universe, as required.

4. DATA AND RESULTS

We use a modified version of `CLASS`¹ Blas et al. (2011) and `hi_class`² Bellini et al. (2020); Zumalacárregui et al. (2017) to elaborate the cosmological evolution of the different models, both at the background and linearly-perturbed levels. In order to confront the models with the data, we use the version of `CLASS` and `hi_class` alongside the public cosmological sampler `MontePython`³ Brinckmann & Lesgourges (2018); Audren et al. (2013) to perform a Monte Carlo Markov chain (MCMC) analysis, with the Gelman-Rubin diagnostic $R - 1 < 0.02$ as our convergence criteria.

Table 1. Parameters and priors used in the analysis. All priors are flat in the ranges given.

Model	Parameter	Default	Prior
Base	ω_b	—	$\mathcal{U}[0.005, 0.1]$
	ω_{cdm}	—	$\mathcal{U}[0.001, 0.99]$
	$100\theta_{\text{MC}}$	—	$\mathcal{U}[0.5, 10]$
	$\ln(10^{10} A_s)$	—	$\mathcal{U}[1.61, 3.91]$
	n_s	—	$\mathcal{U}[0.8, 1.2]$
	τ	—	$\mathcal{U}[0.01, 0.8]$
	M	0	$\mathcal{U}[-5, 5]$
DE	w_0 or w	-1	$\mathcal{U}[-3, 1]$
	w_a	0	$\mathcal{U}[-3, 2]$
PPF	$\log_{10} c_s^2$	0	$\mathcal{U}[-8, 0]$
EFT	c_K	0	$\mathcal{U}[-10, 10]$
	c_B	0	$\mathcal{U}[-10, 10]$
	c_M	0	$\mathcal{U}[-10, 10]$

All the analyses presented in the following have a common set of cosmological parameters, namely: the fractional energy density of cold dark matter and baryons, respectively $\omega_c \equiv \Omega_c h^2$ and $\omega_b \equiv \Omega_b h^2$; the approximation to the acoustic angular scale $\theta_*, \theta_{\text{MC}}$; the amplitude A_s and spectral index n_s of the initial curvature perturbation; and the effective optical depth τ . For all these parameters we use uninformative flat priors reported in Table 1, which also includes the priors of parameters

specific to each of the studied models. The prior for the Base and dark energy (DE) parameters in Table 1 are the same as in Adame et al. (2025a). Furthermore, following the Planck Collaboration, we treat the neutrinos as two massless and one massive with mass $m_\nu = 0.06$ eV, reproducing $N_{\text{eff}} = 3.044$ Aghanim et al. (2020a).

In addition to cosmological and model parameters, we also sample the recommended nuisance parameters for each data likelihood. As we described in the previous sections, for the dark energy perturbations we work within the PPF or the EFT framework. Finally, due to the fact that we need to consider very small sound speed values, following the Planck Collaboration Ade et al. (2016) for the PPF approach we choose to constrain $\log_{10} c_s^2$ instead of c_s^2 .

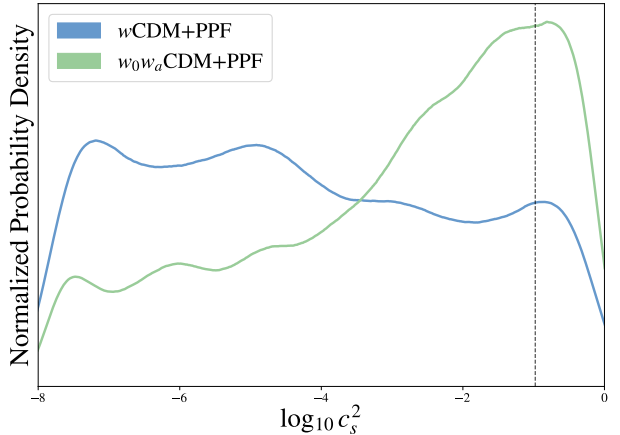


Figure 1. Normalized marginalized 1D posteriors for $\log_{10} c_s^2$, for $w\text{CDM}+\text{PPF}$ and $w_0w_a\text{CDM}+\text{PPF}$ using $\text{BAO}+\text{CMB}+\text{SNe}$ datasets. The dashed line represents the the Maximum A Posteriori (MAP) value $\log_{10} c_s^2 = -0.9780$ for $w_0w_a\text{CDM}$ model, marginalized using `procol`.

4.1. Data

We leverage the latest cosmological observations to place stringent constraints on the dark energy speed of sound. These are briefly described below.

CMB: Our analysis incorporates the full Planck 2018 Cosmic Microwave Background (CMB) data Aghanim et al. (2020a), including the temperature (TT), polarization (EE), and cross (TE) correlation spectra. We utilize the `simall`, `Commander`, and `plik` (for $\ell \geq 30$) likelihoods Aghanim et al. (2020b). This CMB dataset is complemented by Planck CMB lensing potential measurement Aghanim et al. (2020c).

SNe: We incorporate the Union3 sample of Type Ia supernovae (SNe Ia) Rubin et al. (2023). This dataset comprises 2087 SNe Ia, standardized and compiled within the Unity 1.5 Bayesian framework. The

¹ https://github.com/lesgourg/class_public

² https://github.com/miguelzuma/hi_class_public

³ https://github.com/brinckmann/montepython_public

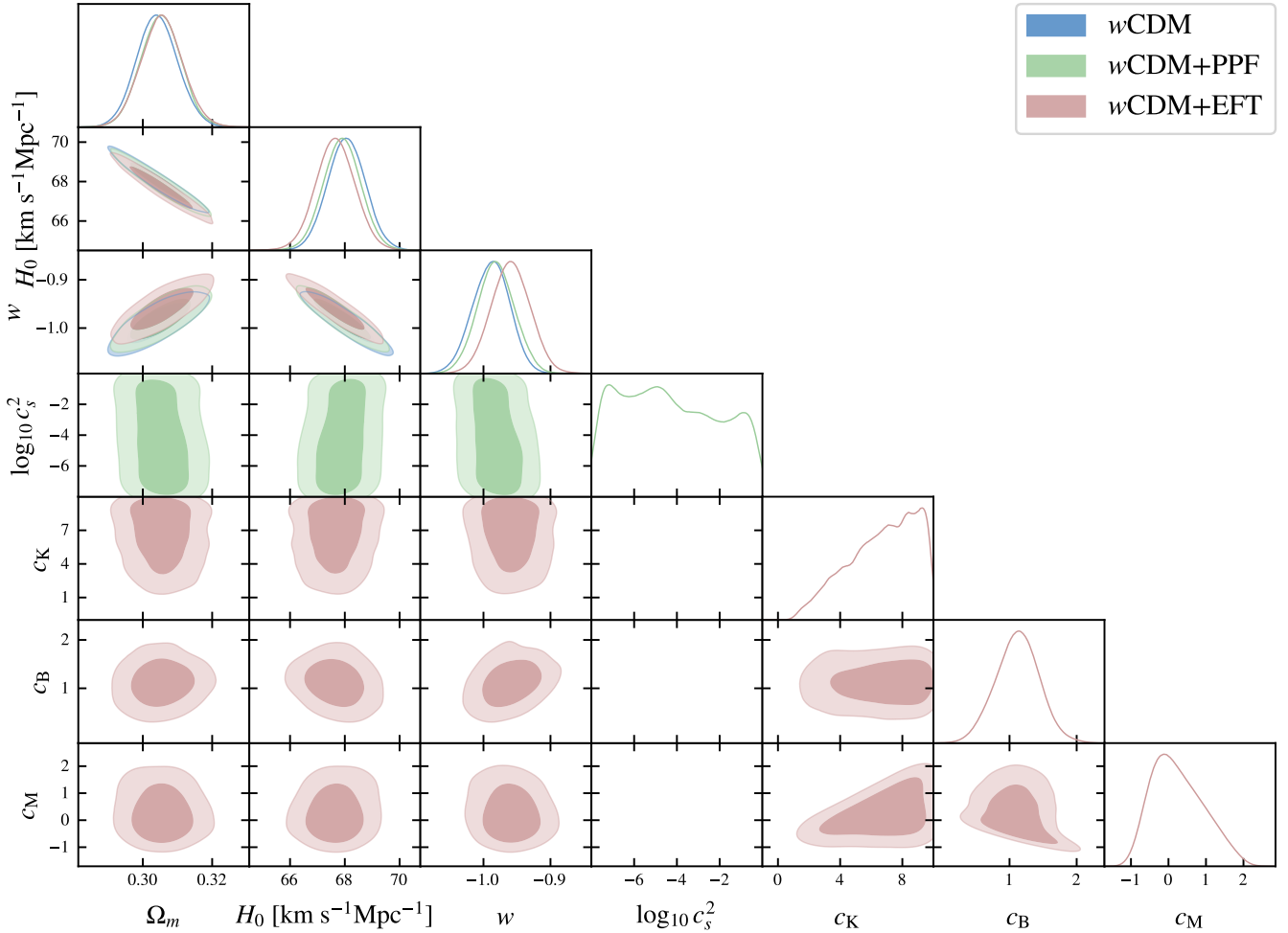


Figure 2. Constraints on w CDM model under Parameterized Post-Friedmann (PPF) and Effective Field Theory (EFT) perturbation descriptions, using BAO+CMB+SNe datasets. The contours represent the 68% and 95% credible intervals. The results are summarized in Table 2.

Hubble diagram is constructed using a quadratic spline interpolation with 22 nodes across the redshift range $0.05 < z < 2.26$. In our analysis, the absolute magnitude M is treated as a free nuisance parameter. As the supernova fluxes are empirically calibrated, the constrained value of M effectively represents an offset from the pre-calibrated baseline.

BAO: We incorporate the latest baryon acoustic oscillation (BAO) measurements from the DESI Data Release 2 (DR2) [Abdul Karim et al. \(2025\)](#). This dataset provides unprecedented precision across a wide redshift range, utilizing multiple tracers: the Bright Galaxy Sample (BGS; $0.1 < z < 0.4$), Luminous Red Galaxies (LRGs; $0.4 < z < 1.1$), Emission Line Galaxies (ELGs; $1.1 < z < 1.6$), Quasars (QSOs; $0.8 < z < 2.1$), and the Lyman- α Forest ($1.77 < z < 4.16$).

4.2. Results and discussion

Let us now present the constraints on dark energy perturbations obtained using BAO+CMB+SNe datasets. We use `procoli`⁴[Karwal et al. \(2024\)](#) to investigate the projection effects, by comparing the Maximum A Posteriori (MAP) values to the mean values of posteriors within the w_0w_a CDM+PPF framework, and `GetDist`⁵[Lewis \(2025\)](#) to make the figures.

4.2.1. Constraints from PPF dark energy perturbations

We find that including PPF dark energy perturbations has only a minor effect on the background cosmological parameters, shifting their values slightly without altering the overall constraints substantially. Since both BAO and SNe Ia primarily constrain the background expansion history, the constraints on dark energy per-

⁴ <https://github.com/tkarwal/procoli/tree/main>

⁵ <https://github.com/cmbant/getdist>

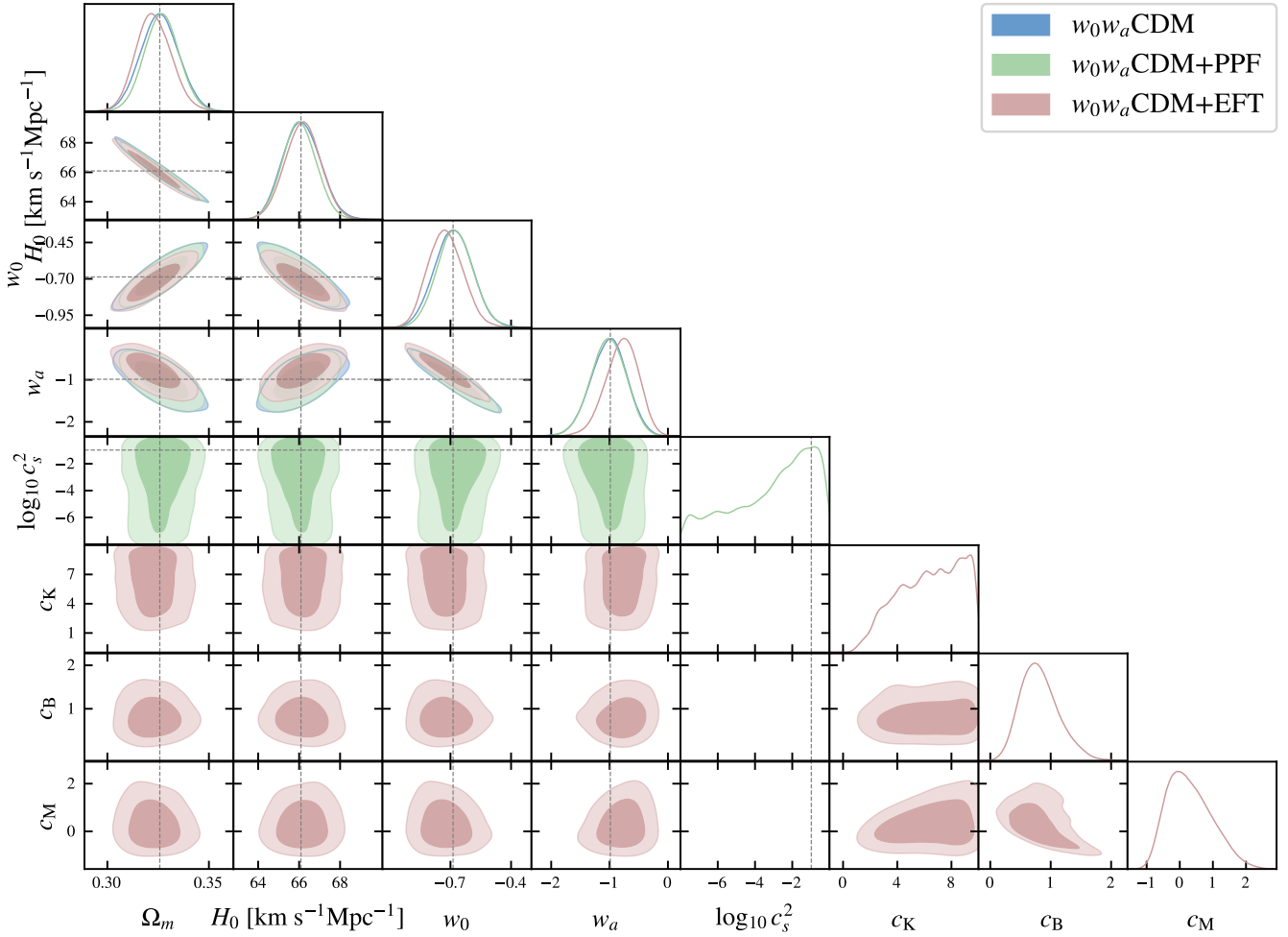


Figure 3. Constraints on w_0w_a CDM model under Parameterized Post-Friedmann (PPF) and Effective Field Theory (EFT) perturbation descriptions, using BAO+CMB+SNe datasets. The contours represent the 68% and 95% credible intervals. The results are summarized in Table 2. Additionally, the dashed lines represent the Maximum A Posteriori (MAP) values for w_0w_a CDM+PPF, namely $\Omega_m = 0.3258$, $H_0 = 66.09 \text{ km s}^{-1} \text{ Mpc}^{-1}$, $w_0 = -0.6871$, $w_a = -0.9867$, $\log_{10} c_s^2 = -0.9780$, marginalized using `procol`.

turbations are driven almost entirely by CMB data, and in particular by the large-scale temperature and polarization power spectra. However, due to the significant uncertainty in large-scale CMB observations, the current data cannot tightly constrain c_s^2 or rule out the $c_s^2 = 1$ case with high confidence.

In Fig. 1 we depict the normalized marginalized 1D posteriors for $\log_{10} c_s^2$ using the PPF approach. Additionally, in Figs. 2 and 3 we present the constraints on the w CDM and w_0w_a CDM model from BAO+CMB+SNe, within the PPF approach, and in Table 2 we summarize the results. As we observe, for the w CDM+PPF case, the sound speed is nearly unconstrained. Nevertheless, in the w_0w_a CDM+PPF scenario, the posterior distributions prefer values below zero, indicating a small sound speed, with the constraint $\log_{10} c_s^2 = -3.00^{+2.9}_{-0.99}$. Using `procol` to exam-

ine projection effects, we find a MAP value of $\log_{10} c_s^2 = -0.9780$, corresponding to $c_s^2 \simeq 0.1052$. This value lies well within the 1σ region, indicating that projection-induced biases remain minimal Adame et al. (2025b) and supporting the robustness of our sound-speed constraints.

This behavior is expected since the clustering effect of dark energy scales as $(1 + w_{de})$ in the Poisson equation. When $(1 + w_{de}) \rightarrow 0$, even very small c_s^2 leaves almost no observable effect. Thus, for the w CDM model, where w is close to -1 , the sound speed remains poorly constrained. In contrast, in the w_0w_a CDM model the degeneracy between $(1 + w_{de})$ and c_s^2 is partially broken, yielding tighter constraints. We emphasize that this improvement is driven by the w_0w_a parameterization rather than the PPF framework itself. This ex-

Table 2. Summary of cosmological parameter constraints from different dataset combinations, for Λ CDM, w CDM model and w_0w_a CDM models, under Parameterized Post-Friedmann (PPF) and Effective Field Theory (EFT) perturbation descriptions. In each case we show the marginalized posterior means and the 68% credible intervals.

Model	Ω_m	H_0 [$\text{km s}^{-1} \text{Mpc}^{-1}$]	w_0 or w	w_a	$\log_{10} c_s^2$	c_K	c_B	c_M
Λ CDM	$0.3020^{+0.0038}_{-0.0038}$	$68.33^{+0.30}_{-0.30}$	—	—	—	—	—	—
w CDM	$0.3042^{+0.0059}_{-0.0059}$	$68.06^{+0.68}_{-0.68}$	$-0.989^{+0.028}_{-0.028}$	—	—	—	—	—
w CDM+PPF	$0.3052^{+0.0059}_{-0.0059}$	$67.90^{+0.69}_{-0.69}$	$-0.981^{+0.028}_{-0.028}$	—	$-4.3^{+2.3}_{-2.3}$	—	—	—
w CDM+EFT	$0.3055^{+0.0060}_{-0.0060}$	$67.65^{+0.72}_{-0.72}$	$-0.959^{+0.029}_{-0.029}$	—	—	$6.7^{+3.0}_{-1.2}$	$1.12^{+0.33}_{-0.33}$	$0.25^{+0.55}_{-0.86}$
w_0w_a CDM	$0.3258^{+0.0093}_{-0.0093}$	$66.12^{+0.90}_{-0.90}$	$-0.685^{+0.093}_{-0.093}$	$-1.01^{+0.30}_{-0.30}$	—	—	—	—
w_0w_a CDM+PPF	$0.3264^{+0.0091}_{-0.0091}$	$66.02^{+0.89}_{-0.89}$	$-0.683^{+0.094}_{-0.094}$	$-0.996^{+0.31}_{-0.31}$	$-3.00^{+2.9}_{-0.99}$	—	—	—
w_0w_a CDM+EFT	$0.3229^{+0.0087}_{-0.0087}$	$66.18^{+0.86}_{-0.86}$	$-0.724^{+0.081}_{-0.092}$	$-0.79^{+0.30}_{-0.25}$	—	$6.4^{+3.4}_{-2.1}$	$0.82^{+0.25}_{-0.37}$	$0.30^{+0.51}_{-0.83}$

plains why DESI+Planck can constrain the w_0w_a CDM sound speed but not the w CDM one.

4.2.2. EFT constraints on dark energy perturbations

We now discuss the results obtained using the EFT framework. In Figs. 2 and 3 we show the constraints on the w CDM model from BAO+CMB+SNe, within the EFT approach, and in Table 2 we summarize the results. The coefficient c_K remains largely unconstrained in both models, consistent with previous studies Bellini et al. (2016); Reischke et al. (2019); Gleyzes et al. (2016); Alonso et al. (2017); Yang et al. (2019); Pan et al. (2019). Although c_K has minimal impact on other cosmological constraints Bellini et al. (2016), we keep it free to ensure compliance with the physical requirement $0 < c_s^2 \leq 1$.

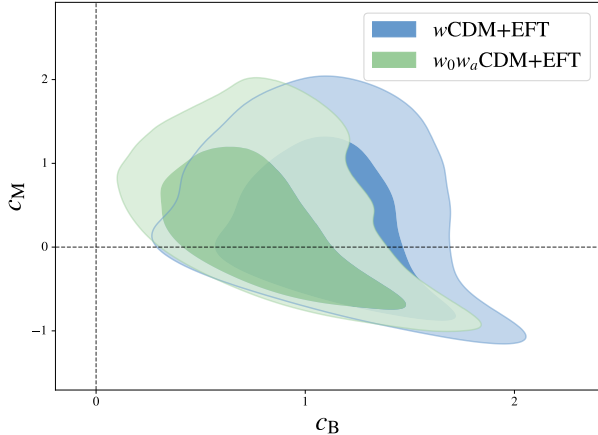


Figure 4. 2D posterior distributions for the EFT coefficients c_M and c_B , for w CDM+EFT and w_0w_a CDM+EFT using BAO+CMB+SNe datasets.

Fig. 4 shows the marginalized posterior of c_M and c_B for w CDM+EFT and w_0w_a CDM+EFT. The region $c_M < 0$ and $c_B < 0$ is excluded by gradient instabilities. The results mildly prefer a nonzero braiding parameter c_B , while remaining consistent with no running of the

Planck mass ($\alpha_M = 0$) or no coupling between dark energy field and spacetime. These constraints are mainly driven by the late ISW effect, since α_M and α_B modify the late-time evolution of the metric potentials. The data prefer $c_B > 0$ and $c_M < 2$, consistent with expectations from CMB-galaxy cross-correlations Stölzner et al. (2018); Seraille et al. (2024). Different background expansion histories have almost no impact on EFT parameter constraints.

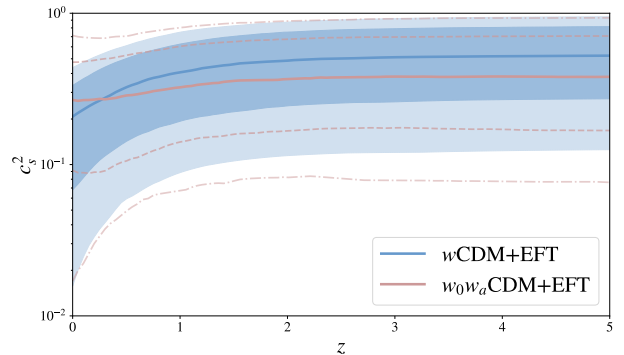


Figure 5. Comparison of the reconstructed sound speed square of dark energy c_s^2 between w CDM+EFT and w_0w_a CDM+EFT, using BAO+CMB+SNe datasets. The w CDM+EFT reconstruction is shown in blue, accompanied by shaded 68% and 95% confidence intervals. While the w_0w_a CDM+EFT is shown in green, the green dashed curve and green dot-dashed curve represent 68% and 95% confidence intervals, respectively. Additionally, both solid curves represent the mean values. Finally, the reconstruction is truncated at $z = 5$ since Ω_{de} becomes negligible at higher redshift.

4.2.3. Reconstruction of the sound speed in EFT

In Fig. 5, using Eq. 8 we reconstruct the evolution of c_s^2 for both w CDM+EFT and w_0w_a CDM+EFT, with 68% and 95% confidence intervals. In both cases the reconstructed sound speed is similar, with mean val-

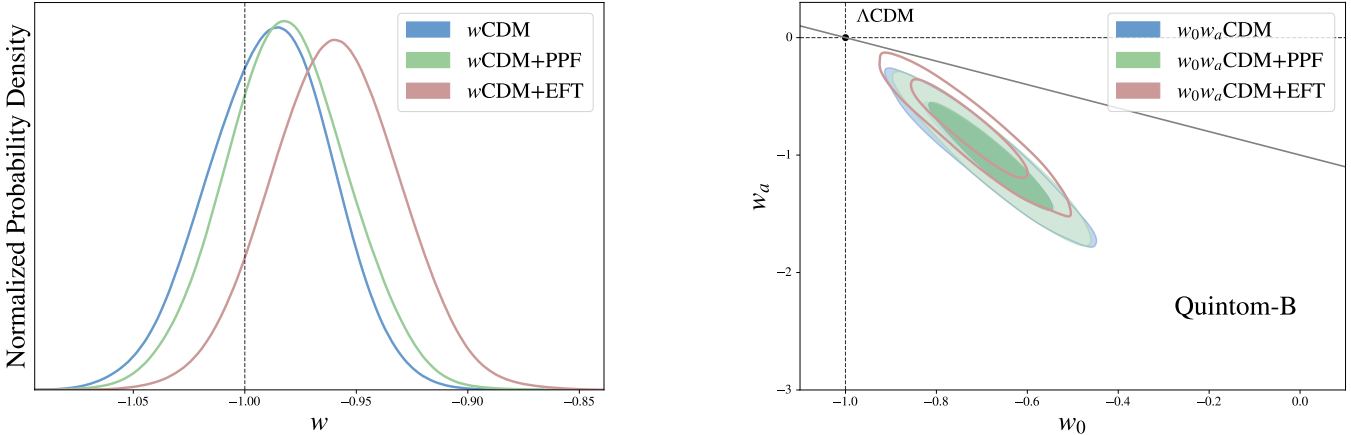


Figure 6. Left panel: the normalized marginalized 1D posterior distribution for w in a w CDM background cosmology under different perturbation descriptions, using BAO+CMB+SNe datasets, where the dashed line represents the Λ CDM paradigm. Right panel: The results for the posterior distributions of w_0 and w_a for w_0w_a CDM model under different perturbation descriptions, using BAO+CMB+SNe datasets. The contours enclose 68% and 95% of the posterior probability. The gray solid line indicates $w_0 + w_a = -1$, while the Λ CDM paradigm ($w_0 = -1$, $w_a = 0$) lies at their intersection. The significance of deviation from Λ CDM scenario is 3.42σ , 3.63σ and 3.19σ for w_0w_a CDM, w_0w_a CDM+PPF and w_0w_a CDM+EFT, respectively.

ues around $0.3 - 0.4$. Since dark energy is negligible at high redshifts, we plot the reconstruction only up to $z = 5$. The evolution observed in Fig. 5 arises from the parametrization $\alpha_i(z) \propto \Omega_{\text{de}}(z)$ of (9). As z increases, $\alpha_i \rightarrow 0$, reproducing the standard quintessence behavior during matter domination ($c_s^2 = 1$) Ratra & Peebles (1988); Wetterich (1988).

4.2.4. Constraints on the equation of state

Fig. 6 compares the reconstructed dark energy equation of state for different models. The left panel shows the marginalized means and 68% confidence intervals for w CDM with different perturbation treatments. The w CDM and w CDM+PPF results are almost identical, while w CDM+EFT predicts a higher value of w .

The right panel shows the constraints on (w_0, w_a) for the w_0w_a CDM model. The gray dashed line indicates $w_0 + w_a = -1$. For both the PPF and EFT approaches, the contours lie below this line, demonstrating the quintom-B behavior: phantom-like at early times and quintessence-like at late times. We also find a 3.42σ deviation from Λ CDM for w_0w_a CDM, increasing slightly to 3.63σ with PPF and decreasing to 3.19σ with EFT. Note the significance of rejection of Λ CDM for w_0w_a CDM is different from the value reported with same data combination in Abdul Karim et al. (2025), these differences arise from the different CMB likelihoods.

4.2.5. Summary of constraints and model comparison

In Table 2 we summarize the marginalized constraints described above, namely the full cosmological parameter distributions for all models and perturbation schemes

presented in Figs. 2–3. In order to objectively assess which models are preferred by the data, we compute the Akaike Information Criterion (AIC) and Bayesian Information Criterion (BIC): i.e. $\text{AIC} = -2 \ln \mathcal{L}_{\text{max}} + 2p_{\text{tot}}$ and $\text{BIC} = -2 \ln \mathcal{L}_{\text{max}} + p_{\text{tot}} \ln N_{\text{tot}}$, where $\ln \mathcal{L}_{\text{max}}$ represents the maximum likelihood of the model and p_{tot} and N_{tot} represent the total number of free parameters and data points respectively Liddle (2007); Anagnostopoulos et al. (2019). We display the corresponding results in Table 3. As we see, the w_0w_a model is slightly favored by AIC, especially without clustering effects. However, BIC continues to prefer Λ CDM, as expected due to its stronger penalty on model complexity.

Table 3. The information criteria AIC and BIC values, for different models with different data combinations. Additionally, we display the differences $\Delta\text{AIC} = \text{AIC}_{\text{model}} - \text{AIC}_{\Lambda\text{CDM}}$, and $\Delta\text{BIC} = \text{BIC}_{\text{model}} - \text{BIC}_{\Lambda\text{CDM}}$.

Model	AIC	BIC	ΔAIC	ΔBIC
Λ CDM	2879.90	3041.49	0	0
w CDM	2882.18	3049.54	2.28	8.05
w CDM+PPF	2882.00	3055.13	2.10	13.64
w CDM+EFT	2878.84	3063.51	-1.06	22.02
w_0w_a CDM	2870.54	3043.67	-9.36	2.18
w_0w_a CDM+PPF	2872.16	3051.06	-7.71	9.57
w_0w_a CDM+EFT	2870.82	3061.27	-9.08	19.78

5. CONCLUSIONS

Recent cosmological observations, and in particular the DESI DR2 BAO measurements, arise a challenge

to the standard Λ CDM paradigm, and strongly suggest that dark energy may exhibit dynamical behavior. Once dark energy is allowed to evolve in time, its perturbations and clustering properties necessarily become part of the physical description: a consistent treatment must go beyond the background level and incorporate the sound speed and stability conditions of the perturbations.

In this work we investigated dark energy perturbations using two complementary frameworks: the Parameterized Post-Friedmann (PPF) approach, which provides a stable description across the phantom divide and regulates the divergence problem of parameterized equation of state models, and the Effective Field Theory (EFT) approach, which offers a unified and model-independent parameterization of perturbations through the α -basis. Using the DESI DR2 BAO data in combination with Planck 2018 CMB and Union3 supernovae, we constrained the clustering behavior of dynamical dark energy and, and in particular its effective sound speed.

Within the PPF framework, we focused on $\log_{10} c_s^2$ to resolve the regime of extremely small sound speeds. For the w CDM model, the sound speed remains essentially unconstrained, as expected for an equation of state close to -1 . However, in the $w_0 w_a$ CDM model, the degeneracy between $(1+w)$ and c_s^2 is broken, yielding the constraint

$$\log_{10} c_s^2 = -3.00^{+2.9}_{-0.99},$$

with a MAP value $\log_{10} c_s^2 = -0.9780$. These results indicate a preference for a small sound speed, but remain broadly consistent with a smooth dark-energy component.

Within the EFT framework we found that α_K is poorly constrained, in agreement with previous studies, whereas the reconstructed sound speed prefers values in the range $c_s^2 \sim 0.3\text{--}0.4$. The parameters α_B and α_M are primarily constrained through their impact on the late-time evolution of gravitational potentials and the ISW effect, and they remain compatible with no running of the Planck mass. Furthermore, we quantified the deviation from Λ CDM in the $w_0 w_a$ CDM background, finding 3.42σ for the background-only model, increasing to 3.63σ when PPF perturbations are included and decreasing to 3.19σ in the EFT case. Finally, a model comparison using AIC and BIC indicates that the $w_0 w_a$ CDM model without clustering effects is most favored by AIC, while BIC, which penalizes the extra parameters more strongly, continues to prefer Λ CDM.

While Planck 2015 found the sound speed of dark energy to be essentially unconstrained, our analysis shows

that the combination of DESI DR2, CMB, and supernova data now yields meaningful constraints on the clustering behavior of dynamical dark energy. At present, the data mildly prefer dynamical evolution of the equation of state, yet still favor dark energy that behaves as a nearly smooth component rather than one that significantly clusters. However, due to the sizeable uncertainties in current large-scale CMB measurements, these conclusions remain provisional.

Future high-precision surveys, including DESI full data release, Euclid, LSST, CMB-S4 and SKA, will dramatically improve constraints on both the background and perturbative properties of dark energy. These observations will help determine whether dark energy truly possesses dynamical behavior or clustering effects, or whether the emerging deviations from Λ CDM arise from systematics. A clearer picture of the sound speed, stability conditions, and large-scale behavior of dark energy, will be essential for establishing the physical origin of cosmic acceleration. In summary, our analysis demonstrates that forthcoming precision surveys will decisively determine whether the mild preference for dynamical but non-clustering dark energy persists.

ACKNOWLEDGMENTS

We are grateful to Zhiyu Lu, Linda Blot and Hao Liu for insightful comments. This work was supported in part by the National Key R&D Program of China (2021YFC2203100, 2024YFC2207500), by the National Natural Science Foundation of China (12433002, 12261131497, 92476203), by CAS young interdisciplinary innovation team (JCTD-2022-20), by 111 Project (B23042), by Anhui Postdoctoral Scientific Research Program Foundation (No. 2025C1184), by CSC Innovation Talent Funds, by USTC Fellowship for International Cooperation, and by USTC Research Funds of the Double First-Class Initiative. ENS acknowledges the contribution of the LISA CosWG and the COST Actions and of COST Actions CA21136 “Addressing observational tensions in cosmology with systematics and fundamental physics (CosmoVerse)”, CA21106 “COSMIC WISPer in the Dark Universe: Theory, astrophysics and experiments (CosmicWISPer)”, and CA23130 “Bridging high and low energies in search of quantum gravity (BridgeQG)”. Kavli IPMU is supported by World Premier International Research Center Initiative (WPI), MEXT, Japan.

REFERENCES

Abbott, B. P., et al. 2017, *Astrophys. J. Lett.*, 848, L13, doi: [10.3847/2041-8213/aa920c](https://doi.org/10.3847/2041-8213/aa920c)

Abdul Karim, M., et al. 2025, *Phys. Rev. D*, 112, 083515, doi: [10.1103/tr6y-kpc6](https://doi.org/10.1103/tr6y-kpc6)

Adame, A. G., et al. 2025a, *JCAP*, 02, 021, doi: [10.1088/1475-7516/2025/02/021](https://doi.org/10.1088/1475-7516/2025/02/021)

—. 2025b, *JCAP*, 09, 008, doi: [10.1088/1475-7516/2025/09/008](https://doi.org/10.1088/1475-7516/2025/09/008)

Ade, P. A. R., et al. 2016, *Astron. Astrophys.*, 594, A14, doi: [10.1051/0004-6361/201525814](https://doi.org/10.1051/0004-6361/201525814)

Aghanim, N., et al. 2020a, *Astron. Astrophys.*, 641, A6, doi: [10.1051/0004-6361/201833910](https://doi.org/10.1051/0004-6361/201833910)

—. 2020b, *Astron. Astrophys.*, 641, A5, doi: [10.1051/0004-6361/201936386](https://doi.org/10.1051/0004-6361/201936386)

—. 2020c, *Astron. Astrophys.*, 641, A8, doi: [10.1051/0004-6361/201833886](https://doi.org/10.1051/0004-6361/201833886)

Alonso, D., Bellini, E., Ferreira, P. G., & Zumalacárregui, M. 2017, *Phys. Rev. D*, 95, 063502, doi: [10.1103/PhysRevD.95.063502](https://doi.org/10.1103/PhysRevD.95.063502)

Anagnostopoulos, F. K., Basilakos, S., & Saridakis, E. N. 2019, *Phys. Rev. D*, 100, 083517, doi: [10.1103/PhysRevD.100.083517](https://doi.org/10.1103/PhysRevD.100.083517)

Audren, B., Lesgourgues, J., Benabed, K., & Prunet, S. 2013, *JCAP*, 1302, 001, doi: [10.1088/1475-7516/2013/02/001](https://doi.org/10.1088/1475-7516/2013/02/001)

Barreira, A., Li, B., Baugh, C., & Pascoli, S. 2014, *JCAP*, 08, 059, doi: [10.1088/1475-7516/2014/08/059](https://doi.org/10.1088/1475-7516/2014/08/059)

Basilakos, S., Paliathanasis, A., & Saridakis, E. N. 2025, *Phys. Lett. B*, 868, 139658, doi: [10.1016/j.physletb.2025.139658](https://doi.org/10.1016/j.physletb.2025.139658)

Basse, T., Bjaelde, O. E., Hannestad, S., & Wong, Y. Y. Y. 2012. <https://arxiv.org/abs/1205.0548>

Batista, R. C. 2021, *Universe*, 8, 22, doi: [10.3390/universe8010022](https://doi.org/10.3390/universe8010022)

Bellini, E., Cuesta, A. J., Jimenez, R., & Verde, L. 2016, *JCAP*, 02, 053, doi: [10.1088/1475-7516/2016/06/E01](https://doi.org/10.1088/1475-7516/2016/06/E01)

Bellini, E., & Sawicki, I. 2014, *JCAP*, 07, 050, doi: [10.1088/1475-7516/2014/07/050](https://doi.org/10.1088/1475-7516/2014/07/050)

Bellini, E., Sawicki, I., & Zumalacárregui, M. 2020, *JCAP*, 02, 008, doi: [10.1088/1475-7516/2020/02/008](https://doi.org/10.1088/1475-7516/2020/02/008)

Bellini, E., & Zumalacárregui, M. 2015, *Phys. Rev. D*, 92, 063522, doi: [10.1103/PhysRevD.92.063522](https://doi.org/10.1103/PhysRevD.92.063522)

Bhattacharyya, A., Alam, U., Pandey, K. L., Das, S., & Pal, S. 2019, *Astrophys. J.*, 876, 143, doi: [10.3847/1538-4357/ab12d6](https://doi.org/10.3847/1538-4357/ab12d6)

Blas, D., Lesgourgues, J., & Tram, T. 2011, *Journal of Cosmology and Astroparticle Physics*, 2011, 034. <https://api.semanticscholar.org/CorpusID:53490516>

Bloomfield, J. K., Flanagan, E. E., Park, M., & Watson, S. 2013, *JCAP*, 08, 010, doi: [10.1088/1475-7516/2013/08/010](https://doi.org/10.1088/1475-7516/2013/08/010)

Brinckmann, T., & Lesgourgues, J. 2018. <https://arxiv.org/abs/1804.07261>

Cai, Y., Ren, X., Qiu, T., Li, M., & Zhang, X. 2025. <https://arxiv.org/abs/2505.24732>

Cai, Y.-F., Saridakis, E. N., Setare, M. R., & Xia, J.-Q. 2010, *Phys. Rept.*, 493, 1, doi: [10.1016/j.physrep.2010.04.001](https://doi.org/10.1016/j.physrep.2010.04.001)

Caldwell, R. R. 2002, *Phys. Lett. B*, 545, 23, doi: [10.1016/S0370-2693\(02\)02589-3](https://doi.org/10.1016/S0370-2693(02)02589-3)

Carroll, S. M., Hoffman, M., & Trodden, M. 2003, *Phys. Rev. D*, 68, 023509, doi: [10.1103/PhysRevD.68.023509](https://doi.org/10.1103/PhysRevD.68.023509)

Chaussidon, E., et al. 2025, *Phys. Rev. D*, 112, 063548, doi: [10.1103/xtql-wh3h](https://doi.org/10.1103/xtql-wh3h)

Chevallier, M., & Polarski, D. 2001, *Int. J. Mod. Phys. D*, 10, 213, doi: [10.1142/S0218271801000822](https://doi.org/10.1142/S0218271801000822)

Chimento, L. P., Forte, M. I., Lazkoz, R., & Richarte, M. G. 2009, *Phys. Rev. D*, 79, 043502, doi: [10.1103/PhysRevD.79.043502](https://doi.org/10.1103/PhysRevD.79.043502)

Cline, J. M., Jeon, S., & Moore, G. D. 2004, *Phys. Rev. D*, 70, 043543, doi: [10.1103/PhysRevD.70.043543](https://doi.org/10.1103/PhysRevD.70.043543)

Creminelli, P., D'Amico, G., Norena, J., & Vernizzi, F. 2009, *JCAP*, 02, 018, doi: [10.1088/1475-7516/2009/02/018](https://doi.org/10.1088/1475-7516/2009/02/018)

De Felice, A., Frusciante, N., & Papadomanolakis, G. 2017, *JCAP*, 03, 027, doi: [10.1088/1475-7516/2017/03/027](https://doi.org/10.1088/1475-7516/2017/03/027)

Deffayet, C., Pujolas, O., Sawicki, I., & Vikman, A. 2010, *JCAP*, 10, 026, doi: [10.1088/1475-7516/2010/10/026](https://doi.org/10.1088/1475-7516/2010/10/026)

Di Valentino, E., et al. 2021, *Astropart. Phys.*, 131, 102604, doi: [10.1016/j.astropartphys.2021.102604](https://doi.org/10.1016/j.astropartphys.2021.102604)

Dinda, B. R., & Banerjee, N. 2024, *Eur. Phys. J. C*, 84, 177, doi: [10.1140/epjc/s10052-024-12547-6](https://doi.org/10.1140/epjc/s10052-024-12547-6)

Efstathiou, G. 2025, *Mon. Not. Roy. Astron. Soc.*, 538, 875, doi: [10.1093/mnras/staf301](https://doi.org/10.1093/mnras/staf301)

Fang, W., Hu, W., & Lewis, A. 2008, *Phys. Rev. D*, 78, 087303, doi: [10.1103/PhysRevD.78.087303](https://doi.org/10.1103/PhysRevD.78.087303)

Feng, B., Wang, X.-L., & Zhang, X.-M. 2005, *Phys. Lett. B*, 607, 35, doi: [10.1016/j.physletb.2004.12.071](https://doi.org/10.1016/j.physletb.2004.12.071)

Giarè, W., Sabogal, M. A., Nunes, R. C., & Di Valentino, E. 2024, *Phys. Rev. Lett.*, 133, 251003, doi: [10.1103/PhysRevLett.133.251003](https://doi.org/10.1103/PhysRevLett.133.251003)

Gleyzes, J., Langlois, D., Mancarella, M., & Vernizzi, F. 2016, *JCAP*, 02, 056, doi: [10.1088/1475-7516/2016/02/056](https://doi.org/10.1088/1475-7516/2016/02/056)

Gleyzes, J., Langlois, D., Piazza, F., & Vernizzi, F. 2013, *JCAP*, 08, 025, doi: [10.1088/1475-7516/2013/08/025](https://doi.org/10.1088/1475-7516/2013/08/025)

Goh, L. W. K., & Taylor, A. N. 2025. <https://arxiv.org/abs/2509.12335>

Gu, G., et al. 2025, doi: [10.1038/s41550-025-02669-6](https://doi.org/10.1038/s41550-025-02669-6)

Gubitosi, G., Piazza, F., & Vernizzi, F. 2013, *JCAP*, 02, 032, doi: [10.1088/1475-7516/2013/02/032](https://doi.org/10.1088/1475-7516/2013/02/032)

Gümrukçüoglu, A. E., Mukohyama, S., & Sotiriou, T. P. 2016, *Phys. Rev. D*, 94, 064001, doi: [10.1103/PhysRevD.94.064001](https://doi.org/10.1103/PhysRevD.94.064001)

Guo, Z.-K., Piao, Y.-S., Zhang, X.-M., & Zhang, Y.-Z. 2005, *Phys. Lett. B*, 608, 177, doi: [10.1016/j.physletb.2005.01.017](https://doi.org/10.1016/j.physletb.2005.01.017)

Horndeski, G. W. 1974, *Int. J. Theor. Phys.*, 10, 363, doi: [10.1007/BF01807638](https://doi.org/10.1007/BF01807638)

Hu, B., Raveri, M., Frusciante, N., & Silvestri, A. 2014. <https://arxiv.org/abs/1405.3590>

Hu, W. 2005, *Phys. Rev. D*, 71, 047301, doi: [10.1103/PhysRevD.71.047301](https://doi.org/10.1103/PhysRevD.71.047301)

—. 2008, *Phys. Rev. D*, 77, 103524, doi: [10.1103/PhysRevD.77.103524](https://doi.org/10.1103/PhysRevD.77.103524)

Karwal, T., Patel, Y., Bartlett, A., et al. 2024. <https://arxiv.org/abs/2401.14225>

Kunz, M., Nesseris, S., & Sawicki, I. 2015, *Phys. Rev. D*, 92, 063006, doi: [10.1103/PhysRevD.92.063006](https://doi.org/10.1103/PhysRevD.92.063006)

Lewis, A. 2025, *JCAP*, 08, 025, doi: [10.1088/1475-7516/2025/08/025](https://doi.org/10.1088/1475-7516/2025/08/025)

Li, C., Cai, Y., Cai, Y.-F., & Saridakis, E. N. 2018, *JCAP*, 10, 001, doi: [10.1088/1475-7516/2018/10/001](https://doi.org/10.1088/1475-7516/2018/10/001)

Li, T.-N., Li, Y.-H., Du, G.-H., et al. 2025, *Eur. Phys. J. C*, 85, 608, doi: [10.1140/epjc/s10052-025-14279-7](https://doi.org/10.1140/epjc/s10052-025-14279-7)

Li, T.-N., Wu, P.-J., Du, G.-H., et al. 2024, *Astrophys. J.*, 976, 1, doi: [10.3847/1538-4357/ad87f0](https://doi.org/10.3847/1538-4357/ad87f0)

Liddle, A. R. 2007, *Mon. Not. Roy. Astron. Soc.*, 377, L74, doi: [10.1111/j.1745-3933.2007.00306.x](https://doi.org/10.1111/j.1745-3933.2007.00306.x)

Linder, E. V. 2003, *Phys. Rev. Lett.*, 90, 091301, doi: [10.1103/PhysRevLett.90.091301](https://doi.org/10.1103/PhysRevLett.90.091301)

Lodha, K., et al. 2025, *Phys. Rev. D*, 112, 083511, doi: [10.1103/w4c6-1r5j](https://doi.org/10.1103/w4c6-1r5j)

Luciano, G. G., Paliathanasis, A., & Saridakis, E. N. 2026, *JHEAp*, 49, 100427, doi: [10.1016/j.jheap.2025.100427](https://doi.org/10.1016/j.jheap.2025.100427)

Ma, C.-P., & Bertschinger, E. 1995, *Astrophys. J.*, 455, 7, doi: [10.1086/176550](https://doi.org/10.1086/176550)

Pan, S., Yang, W., Singha, C., & Saridakis, E. N. 2019, *Phys. Rev. D*, 100, 083539, doi: [10.1103/PhysRevD.100.083539](https://doi.org/10.1103/PhysRevD.100.083539)

Park, M., Zurek, K. M., & Watson, S. 2010, *Phys. Rev. D*, 81, 124008, doi: [10.1103/PhysRevD.81.124008](https://doi.org/10.1103/PhysRevD.81.124008)

Perlmutter, S., et al. 1999, *Astrophys. J.*, 517, 565, doi: [10.1086/307221](https://doi.org/10.1086/307221)

Popovic, B., et al. 2025. <https://arxiv.org/abs/2511.07517>

Pujolas, O., Sawicki, I., & Vikman, A. 2011, *JHEP*, 11, 156, doi: [10.1007/JHEP11\(2011\)156](https://doi.org/10.1007/JHEP11(2011)156)

Ratra, B., & Peebles, P. J. E. 1988, *Phys. Rev. D*, 37, 3406, doi: [10.1103/PhysRevD.37.3406](https://doi.org/10.1103/PhysRevD.37.3406)

Reischke, R., Spurio Mancini, A., Schäfer, B. M., & Merkel, P. M. 2019, *Mon. Not. Roy. Astron. Soc.*, 482, 3274, doi: [10.1093/mnras/sty2919](https://doi.org/10.1093/mnras/sty2919)

Ren, X., Yan, S.-F., Zhao, Y., Cai, Y.-F., & Saridakis, E. N. 2022, *Astrophys. J.*, 932, 131, doi: [10.3847/1538-4357/ac6ba5](https://doi.org/10.3847/1538-4357/ac6ba5)

Riess, A. G., et al. 1998, *Astron. J.*, 116, 1009, doi: [10.1086/300499](https://doi.org/10.1086/300499)

Rubin, D., et al. 2023. <https://arxiv.org/abs/2311.12098>

Sbisà, F. 2015, *Eur. J. Phys.*, 36, 015009, doi: [10.1088/0143-0807/36/1/015009](https://doi.org/10.1088/0143-0807/36/1/015009)

Seraillé, E., Noller, J., & Sherwin, B. D. 2024, *Phys. Rev. D*, 110, 123525, doi: [10.1103/PhysRevD.110.123525](https://doi.org/10.1103/PhysRevD.110.123525)

Stölzner, B., Cuoco, A., Lesgourgues, J., & Bilicki, M. 2018, *Phys. Rev. D*, 97, 063506, doi: [10.1103/PhysRevD.97.063506](https://doi.org/10.1103/PhysRevD.97.063506)

Takada, M. 2006, *Phys. Rev. D*, 74, 043505, doi: [10.1103/PhysRevD.74.043505](https://doi.org/10.1103/PhysRevD.74.043505)

Vikman, A. 2005, *Phys. Rev. D*, 71, 023515, doi: [10.1103/PhysRevD.71.023515](https://doi.org/10.1103/PhysRevD.71.023515)

Wetterich, C. 1988, *Nucl. Phys. B*, 302, 668, doi: [10.1016/0550-3213\(88\)90193-9](https://doi.org/10.1016/0550-3213(88)90193-9)

Wolf, W. J., García-García, C., Anton, T., & Ferreira, P. G. 2025, *Phys. Rev. Lett.*, 135, 081001, doi: [10.1103/jysf-k72m](https://doi.org/10.1103/jysf-k72m)

Xia, J.-Q., Cai, Y.-F., Qiu, T.-T., Zhao, G.-B., & Zhang, X. 2008, *Int. J. Mod. Phys. D*, 17, 1229, doi: [10.1142/S0218271808012784](https://doi.org/10.1142/S0218271808012784)

Yan, S.-F., Zhang, P., Chen, J.-W., et al. 2020, *Phys. Rev. D*, 101, 121301, doi: [10.1103/PhysRevD.101.121301](https://doi.org/10.1103/PhysRevD.101.121301)

Yang, W., Pan, S., Di Valentino, E., Saridakis, E. N., & Chakraborty, S. 2019, *Phys. Rev. D*, 99, 043543, doi: [10.1103/PhysRevD.99.043543](https://doi.org/10.1103/PhysRevD.99.043543)

Yang, Y., Ren, X., Wang, Q., et al. 2024, *Sci. Bull.*, 69, 2698, doi: [10.1016/j.scib.2024.07.029](https://doi.org/10.1016/j.scib.2024.07.029)

Yang, Y., Wang, Q., Li, C., et al. 2025a, *JCAP*, 08, 050, doi: [10.1088/1475-7516/2025/08/050](https://doi.org/10.1088/1475-7516/2025/08/050)

Yang, Y., Wang, Q., Ren, X., Saridakis, E. N., & Cai, Y.-F. 2025b, *Astrophys. J.*, 988, 123, doi: [10.3847/1538-4357/ade43f](https://doi.org/10.3847/1538-4357/ade43f)

Ye, G., Martinelli, M., Hu, B., & Silvestri, A. 2025, *Phys. Rev. Lett.*, 134, 181002, doi: [10.1103/PhysRevLett.134.181002](https://doi.org/10.1103/PhysRevLett.134.181002)

Zhang, X.-F., Li, H., Piao, Y.-S., & Zhang, X.-M. 2006, *Mod. Phys. Lett. A*, 21, 231, doi: [10.1142/S0217732306018469](https://doi.org/10.1142/S0217732306018469)

Zhao, G.-B., Xia, J.-Q., Li, M., Feng, B., & Zhang, X. 2005,
Phys. Rev. D, 72, 123515,
doi: [10.1103/PhysRevD.72.123515](https://doi.org/10.1103/PhysRevD.72.123515)

Zumalacárregui, M., Bellini, E., Sawicki, I., Lesgourgues, J.,
& Ferreira, P. G. 2017, JCAP, 08, 019,
doi: [10.1088/1475-7516/2017/08/019](https://doi.org/10.1088/1475-7516/2017/08/019)